International Journal of Engineering Research and General Science Volume 3, Issue 3, May-June, 2015
ISSN 2091-2730

# Comparison of Seismic Response of an Insulator Bushing using Time History and Response Spectrum Methods

Gargi Sinvhal[#1], G. S. Grewal[*2], V.R. Patel[#3]

[#]Applied Mechanics Department, Maharaja Sayajirao University Baroda, India
[1]gsinvhal@gmail.com
[3]zarnaasso@yahoo.com

[*]Mechanical and Insulating Materials Division, Electrical Research and Development Association Baroda, India
[2]gurpreet.grewal@erda.org

**Abstract**—Experience of past earthquakes has clearly revealed significant damage risk to critical power transmission equipment such as transformers. Specifically, it has been seen that the insulator bushings such as those used on transformer tops are particularly vulnerable to earthquake induced failure. Seismic measurements and qualification of bushings using the seismic testing approach is a time consuming and expensive proposition. This is further compounded by lack of easy availability of six axis seismic machines which meet required mass and volume handling capability of the payload being tested. Consequently, power utilities all over the world usually take recourse to qualification of such power equipment in a virtual environment by the numerical simulation approach using the methodology of Multi Degree of Freedom (MDOF) linear dynamical systems. In the present work, a 33kV insulator bushing has been subjected to virtual seismic analysis using the Finite Element Analysis (FEA). Specifically, the central purpose of this work is to rationalize the preferred use of the approximate "superposition of spectral responses" method as a convenient technique of choice for virtual seismic qualification instead of the exact but more time consuming "time history based modal superposition" method.

**Keywords**—Finite Element Analysis, Insulators, Modal Superposition, Numerical Simulation, Power Transmission, Seismic Measurements, Spectral Responses, Transformers

## INTRODUCTION

An insulator bushing is an insulated device that allows an electrical conductor to pass safely through it and connect to other equipment at its ends. Bushings are one of the most vulnerable components prone to seismic damage. In the event of an earthquake, failure of a bushing may take a transformer out of service, causing severe disruption of electric service [1]. A damaged bushing can be repaired or replaced, but the losses incurred due to failure of the substation owing to the damaged bushing cannot be mended. Further, reinstalling or replacing a bushing is not just an expensive task, but is also time consuming. The failure mode of porcelain bushings include complete fracture of the ceramic material as well as slipping resulting in temporary oil leakages between the flange and the lower porcelain element.
During the 1989 'Loma Prieta' and the 1994 'Northridge' earthquakes, studies on substation equipment, have revealed the poor performance and seismic vulnerability of porcelain bushings and post insulators [2]. Most of the damage during the 'Loma Prieta' earthquake occurred on 230kV and 500kV transformers due to cracks in porcelain bushings, anchorage failures and leakages [3]. Similarly during the 'Northridge' earthquake significant damage occurred due to failure of bushings, anchorages, lightening arresters and conservator tanks [4].

Seismic qualification of insulator bushings is most optimally carried out using the virtual simulation approach based on Finite Element based numerical method for Multi Degree of Freedom (MDOF) linear dynamical systems. In the present work, we have carried out seismic analysis of a 33 kV bushing using two methods. The first method is the exact but time consuming technique of "time history based modal superposition". In contrast, the second method is the approximate "superposition of spectral responses" technique which uses the response spectrum of the equipment being qualified for computing the modal responses. The central idea of this work is to quantify the accuracy of the "superposition of the spectral responses" method with respect to the more exact predictions of the "time history based modal superposition" method.

## THEORY

In this section, we present the essential theoretical background which forms the basis of the "superposition of spectral responses" and the "time history based modal superposition" methods for seismic qualification of equipment/components such as transformer bushings.

### Time History Based Modal Superposition Method

In this method, the coupled multi degree of freedom equations of motion for the equipment/structure are first written as [5]:

$$[M]\{\ddot{u}_t\} + [C]\{\dot{u}_t\} + [K]\{u\} = \{F_{eff}(t)\} \ldots\ldots\ldots\ldots \quad (1)$$

Where:
[M] = Mass matrix
[C] = Damping matrix
[K] = Stiffness matrix
$\{\ddot{u}_t\}, \{\dot{u}_t\}, \{u\}$= Relative acceleration, velocity and displacement vectors respectively
$\{F_{eff}(t)\}$ = Effective force vector

The above coupled MDOF system is decoupled using the modal matrix $[\emptyset]$ to affect transformation between geometrical and generalized coordinates, $\{Z\}$ by:

$$\{Z\} = [\emptyset]\{u\} \ldots\ldots\ldots\ldots\ldots\ldots\ldots\ldots\ldots\ldots\ldots\ldots\ldots\ldots \quad (2)$$

In the above equation, the modal matrix $[\emptyset]$ is obtained by solving the following eigenvalue problem:

$$[K][\emptyset] = [M][\emptyset][\lambda] \ldots\ldots\ldots\ldots\ldots\ldots\ldots\ldots\ldots\ldots\ldots \quad (3)$$

Where:
$[\lambda]$ = Diagonal matrix with elements $\omega_i{}^2$, also obtained from Eq. (3).

The n uncoupled single degree of freedom equations are subsequently obtained as (for i = 1 to n):

$$\ddot{Z}_i(t) + 2\xi_i\omega_i\dot{Z}_t(t) + \omega_i{}^2 Z_i(t) = -\frac{\Delta_i}{\hat{m}_i}\ddot{u}_g(t) \ldots\ldots\ldots\ldots\ldots\ldots \quad (4)$$

Where:
$\ddot{Z}_i(t), \dot{Z}_t(t), Z_i(t)$ = Generalized acceleration, velocity and displacement for $i^{th}$ mode, respectively
$\xi_i$ = Damping ratio for $i^{th}$ mode
$\omega_i$ = Natural frequency of $i^{th}$ mode
$\hat{m}_i$ = Generalized mass related to the $i^{th}$ mode= $\{\emptyset_i\}^T [M] \{\emptyset_i\}$
$\ddot{u}_g(t)$ = ground acceleration

$\Delta_i$ is obtained through the loading related to ith mode, $\tilde{P}_i(t)$ by

$$\tilde{P}_i(t) = \{\emptyset_i\}^T\{F_{eff}\} = -\{\emptyset_i\}^T [M]\{I\}\ddot{u}_g(t) \ldots\ldots\ldots\ldots \quad (5)$$

Where:
{I} = influence vector

The n uncoupled equations represented by Eq. (4) are solved by direct Duhamel integral to give:

$$Z_i(t) = \frac{\Delta_i}{\hat{M}_i}\left[\left(\frac{-1}{\omega_i}\right)\int_0^t \ddot{u}_g(t)[e^{-\xi_i\omega_i(t-\tau)}]\sin\left\{\omega_{Di}\sqrt{1-\varsigma^2}(t-\tau)\right\}d\tau\right] \ldots\ldots\ldots\ldots\ldots\ldots\ldots\ldots\ldots\ldots\ldots\ldots\ldots\ldots\ldots\ldots\ldots\ldots \quad (6)$$

$$\Rightarrow Z_i(t) = \frac{\Delta_i}{\hat{M}_i}\left(D_i(t)\right) \ldots\ldots\ldots\ldots\ldots\ldots\ldots\ldots\ldots\ldots\ldots\ldots \quad (7)$$

Where:

$$D_i(t) = \text{Duhamel's integral} = \left(\frac{-1}{\omega_i}\right)\int_0^t \ddot{u}_g(t)[e^{-\xi_i\omega_i(t-\tau)}]\sin\left\{\omega_{Di}\sqrt{1-\varsigma^2}(t-\tau)\right\}d\tau \ldots\ldots\ldots\ldots \quad (8)$$

$$\omega_{Di} = \omega_i\sqrt{1-\xi_i{}^2} \ldots\ldots\ldots\ldots\ldots\ldots\ldots\ldots\ldots\ldots\ldots\ldots\ldots \quad (9)$$

It is to be noted that for lightly damped systems ($\xi_i < 0.20$), $\omega_{Di} \cong \omega_i$

Having obtained the generalized response for each mode, the overall response in the geometric coordinates is simply obtained by the linear transform:

$$\{u(t)\} = [\emptyset]\{Z(t)\} = [\emptyset]\left\{\frac{\Delta_i}{\widehat{M}_i} D_i(t)\right\} \quad \ldots\ldots\ldots\ldots\ldots \quad (10)$$

Subsequently, the total geometric relative response is converted into elastic force vector $\{E_f\}$ through the standard equation for linear elastic structure as:

$$\{E_f\} = [K]\{u(t)\} = [K][\emptyset]\{Z(t)\} = [M][\emptyset][\lambda]\{Z(t)\} = [M][\emptyset]\left\{\frac{\Delta_i}{\widehat{M}_i}\omega_i{}^2 D_i(t)\right\} \ldots\ldots\ldots\ldots \quad (11)$$

Finally, Eq. (11) is converted into the stress tensor through linear elastic stress analysis and the stress and strain tensors, displacement vector field along with various structural invariants are plotted as a function of the geometric coordinates.

### Superposition of Spectral Responses Method

This method approximates the full response generated by method given in A. Essentially; it directly uses the design response spectrum used for qualification of the equipment to obtain the maximum response for each of n uncoupled SDOF systems that characterize the equipment.

In other words, the maximum response in generalized coordinates is simply obtained for each i[th] mode as:

$$(Z_i)_{max} = \left[\frac{\Delta_i}{\widehat{M}_i}\right]\theta_{design}\left(\xi_i, \omega_i\right) \ldots\ldots\ldots\ldots\ldots\ldots\ldots\ldots\ldots\ldots \quad (12)$$

In the geometric coordinate system, the above equation leads to the expression for maximum displacement of the ith mode as:

$$(u_i)_{max} = \left[\emptyset_i \frac{\Delta_i}{\widehat{M}_i}\right]\theta_{design}\left(\xi_i, \omega_i\right) \ldots\ldots\ldots\ldots\ldots\ldots\ldots\ldots \quad (13)$$

The above maximum modal responses for the n uncoupled modes to the design response spectrum $\theta_{design}\left(\xi_i, \omega_i\right)$ are subsequently combined into the total response using modal combination techniques. There are various mode combination methods used widely. In the present work, three popular methods have been used. These methods are square root sum of squares (SRSS), complete quadratic combination (CQC) and Rosenblueth method (ROSE). The relevant expressions for these methods are summarized below:

1) *Square Root Sum of Squares Method (SRSS)*: In the square root sum of squares method, the peak responses are evaluated using the following expression [6]:

$$r_{max} = \sqrt{\sum_{i=1}^{n} r_i{}^2} \quad \ldots\ldots\ldots\ldots\ldots\ldots\ldots\ldots\ldots\ldots\ldots\ldots \quad (14)$$

*Where*:

$r_i$ = Response of i[th] mode

$r_{max}$ = Maximum response

2) *Rosenblueth Method (ROSE):* Based on the application of random vibration theory, this method of mode combination uses a more practical approach. A correlation factor is used which takes into account the mode interactions. Hence the modal responses with presence of close spaced natural frequencies can be evaluated accurately. The relevant equation can be written as below [7]:

$$r_{max} = \sqrt{\sum_{i=1}^{n}\sum_{j=1}^{n} r_i \rho_{ij} r_j} \quad \ldots\ldots\ldots\ldots\ldots\ldots\ldots\ldots\ldots\ldots\ldots \quad (15)$$

*Where*:

$r_i$ & $r_j$ = Peak responses for the i[th] and j[th] modes, respectively

$\rho_{ij}$ = Correlation coefficient between the i[th] and j[th] modes

$$\rho_{ij} = \frac{1}{1 + \left(\frac{\omega_i' - \omega_j'}{\varsigma_i'\omega_i + \varsigma_j'\omega_j}\right)^2} \quad \ldots\ldots\ldots\ldots\ldots\ldots\ldots\ldots \quad (16)$$

$Where$:

$\omega_i \; and \; \omega_j$ = Undamped natural frequencies for the i[th] and j[th] modes respectively.

$\omega_i' \; and \; \omega_j'$ = Damped natural frequencies for the i[th] and j[th] modes, respectively.

$\varsigma_i$ = Damping ratio for the i[th] mode

$\varsigma_i'$ = Modified damping ratio for the i[th] mode

The relationships between modified and raw natural frequencies as well as modified and raw damping ratios are given as:

$$\omega_i' = \omega_i(1 - \varsigma_i^2)^{\frac{1}{2}} \quad \ldots\ldots\ldots\ldots\ldots\ldots\ldots\ldots\ldots\ldots\ldots \quad (17)$$

$$\varsigma_i' = \varsigma_i + \left(\frac{2}{t_D\omega_i}\right) \quad \ldots\ldots\ldots\ldots\ldots\ldots\ldots\ldots\ldots\ldots\ldots \quad (18)$$

$Where$:

$t_D$ = Earthquake duration

3) *Complete Quadratic Combination (CQC):* This method which is similar to the ROSE method is again based on the application of random vibration theory. The basic CQC expression can be written as [8-9]:

$$r_{max} = \sqrt{\sum_{i=1}^{n}\sum_{j=1}^{n} r_i\rho_{ij}r_j} \quad \ldots\ldots\ldots\ldots\ldots\ldots\ldots\ldots\ldots\ldots \quad (19)$$

$Where$:

$r_i$ & $r_j$ = Peak responses for the i[th] and j[th] modes, respectively

$\rho_{ij}$ = Correlation coefficient between the i[th] and j[th] modes

When the damping ratios are different, it can be shown that the correlation coefficient $\rho_{ij}$ is given as [9]:

$$\rho_{ij} = \frac{8(\varsigma_i\varsigma_j)^{\frac{1}{2}}(\varsigma_i + \beta\varsigma_j)\beta^{3/2}}{(1-\beta^2)^2 + 4\varsigma_i\varsigma_j\beta(1+\beta^2) + 4(\varsigma_i{}^2 + \varsigma_j{}^2)\beta^2} \quad \ldots (20)$$

Where:

$\varsigma_i$&$\varsigma_j$ = Damping ratios of the i[th] and j[th] modes, respectively

$\beta = \frac{\omega_j}{\omega_i}$, = $\omega_j \; and \; \omega_i$ are j[th] and i[th] eigenvalues, respectively

When damping ratios for both the modes are the same, the correlation coefficient can be shown to be [9]:

$$\rho_{ij} = \frac{8\varsigma^2(1+\beta)\beta^{3/2}}{(1-\beta^2)^2 + 4\varsigma^2\beta(1+\beta)^2} \quad \ldots\ldots\ldots\ldots\ldots \quad (21)$$

Where:

$\varsigma$ = Modal damping ratio

**SEISMIC ANALYSIS OF BUSHING**

## Background

A 33kV bushing is analysed by the time history and response spectrum analysis methods using the FEM package, ANSYS. ANSYS offers a comprehensive software suite that provides access to virtually any field of engineering simulation that a design process requires [10].

The entire seismic analysis simulation procedure is broadly divided into five parts:

- Modelling
- Meshing
- Natural Frequency Analysis (Modal Analysis)
- Time History Analysis (Transient Analysis)
- Response Spectrum Analysis

### Solid Model of the Insulator Bushing

The 33kV bushing was modelled in SOLIDWORKS as six separate sections. The integrated solid model is shown in Figure 54.

*Figure 54: Solid Model of Bushing*

The material properties assigned to various sections/parts of the bushing are given in Table IX. The interfacial boundary conditions were fixed by assigning interfaces to behave as bonded joints.

*Table IX: ASSIGNED MATERIAL PROPERTIES*

| Part | Material Data | | | |
|---|---|---|---|---|
| | **Material** | **Density (kg/m3)** | **Young's Modulus (Pa)** | **Poisson's Ratio** |
| Brass Bush | Brass | 8450 | 1.05E+11 | 0.34 |
| Inner Conductor | Copper | 8300 | 1.100E+11 | 0.34 |
| Outer Covering | Porcelain | 2400 | 1.000E+11 | 0.17 |

### Meshed Model of the Insulator Bushing

The solid model of the bushing was imported in to the ANSYS package and adaptive meshing was carried out using 29,688 tetrahedral elements and 59,479 nodes. Each tetrahedral element consists of 5 exterior nodes, each with 6 degrees of freedom. The meshed solid model is as shown in Figure 55.

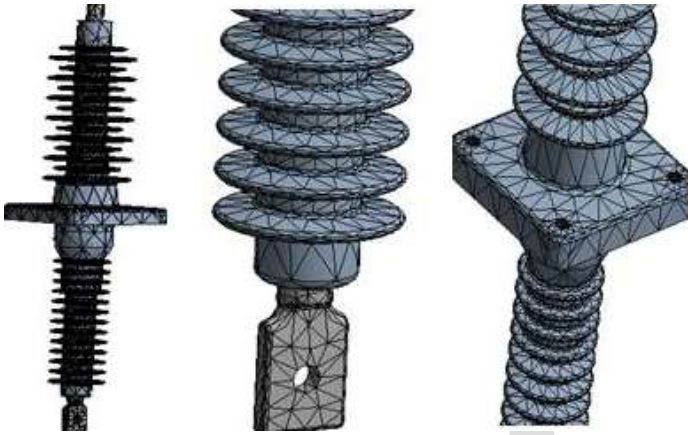

*Figure 55: Meshed Solid Model of Bushing*

### Natural Frequency Analysis

The first step in any virtual seismic analysis is natural frequency analysis, as determination of the system eigenvalues and eigenmodes are required for the dynamical analysis. The eigenvalues (natural) frequencies and eigenmodes are computed by solving the characteristic equation given by Eq. (3).

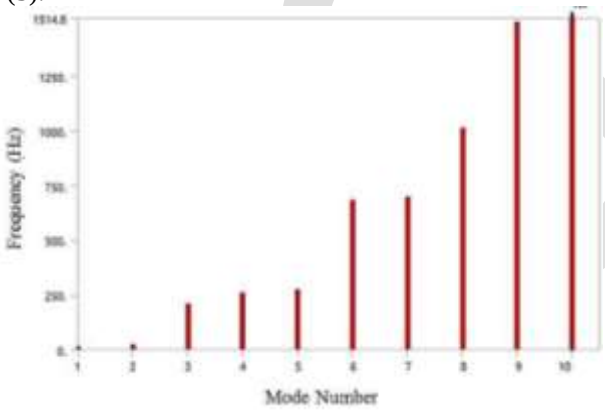


*Figure 56: Frequency versus Mode Number for the First Ten Modes of the Bushing*

*Table X: FIRST TEN NATURAL FREQUENCY VALUES VERSUS MODE NUMBER FOR THE BUSHING*

| Mode | Frequency (Hz) |
|---|---|
| 1 | 15.413 |
| 2 | 22.709 |
| 3 | 209.56 |
| 4 | 259.15 |
| 5 | 272.43 |
| 6 | 682.86 |
| 7 | 698.35 |
| 8 | 1013.7 |
| 9 | 1498.4 |
| 10 | 1514.8 |

The modal frequencies were computed for the first 10 modes. It was observed that the required mass participation ratio of more than 90% was achieved using these 10 modes, making the set sufficiently accurate for the subsequent analysis. Graphical plot of the eigenvalues as a function of mode number are presented in Figure 56 and the natural frequencies values are summarized in Table X.

### Time History Based Modal Superposition Analysis

The time history analysis was conducted using the ELCENTRO (1940) actual time history acceleration data, see Figure 57. Using the transient analysis module of ANSYS version 14.5 based on the framework given in Eqs. (1) to (2).

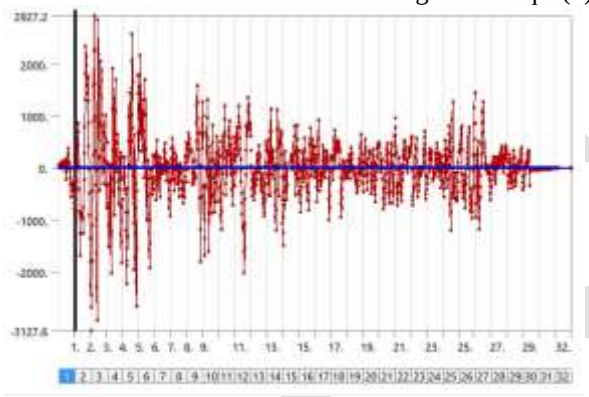

*Figure 57: Acceleration (mm/s2) Versus Time (secs.) for ELCENTRO 1940 Earthquake*

### Superposition of Spectral Responses Analysis

The superposition of spectral response analysis was conducted using all the three methods of mode combination detailed in section II of this paper. The Response Spectra curve for ELCENTRO earthquake of 1940 with 5% damping was used for analysis, Figure 58.

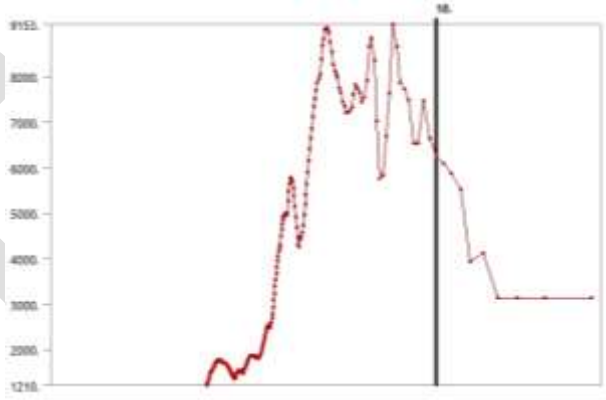

*Figure 58: Acceleration Response Spectrum Curve of Elcentro 1940 Earthquake*

**RESULTS AND DISCUSSIONS**

The results of the "Superposition of Spectral Responses" analysis using the three chosen mode combination methods are compared with the results of the "Time history based modal superposition" analysis in Table XI and Table XII. Specifically in Table III, maximum values of four different stress types namely the equivalent stress, normal stress(X), normal stress(Y) and the shear stress(XY) are presented. It can be seen from Table III that the highest percentage differences of the predictions of the three "Superposition of Spectral Responses" techniques with respect to the mean value are +1%, +1.82%, +1.07%, +0.35% for equivalent stress, normal stress(X), normal stress(Y), shear stress(XY) respectively. Further when the mean values of the SRSS, CQC and ROSE predictions are compared with results of the "time history based modal superposition" method, percentage differences are found as +2.2%, -5.6%, +4.72% and +7.26%, respectively for equivalent stress, normal stress(X), normal stress(Y), shear stress(XY) respectively. Finite element method output plots for equivalent stress, normal stress(X) and shear stress (XY) are presented for reference in Figure 6. Zoom in maps of the equivalent stress in the copper conductor and the porcelain bushing is shown in Figure 7. The data presented in Table III is also plotted as a bar graph in Figure 8.

*Table XI: MAXIMUM STRESS STATE PREDICTIONS*

| Maximum Response | MAXIMUM STRESS (MPa) | | | | Highest % Difference of (A) wrt Mean of (A) | Highest % Difference of (B) wrt Mean of (A) |
|---|---|---|---|---|---|---|
| | Type (A) | | | Type (B) | | |
| | SRSS | CQC | ROSE | Transient | | |
| Equivalent Stress | 28.41 | 28.01 | 27.96 | 28.78 | +1.00 | +2.2 |
| Normal Stress (x) | 10.09 | 9.83 | 9.80 | 9.35 | +1.82 | -5.6 |
| Normal Stress (y) | 25.81 | 25.42 | 25.37 | 26.80 | +1.07 | +4.72 |
| Shear Stress | 5.77 | 5.74 | 5.74 | 6.20 | +0.35 | +7.26 |

Similarly, the results for the deformation prediction using by the three "superposition of spectral responses" methods are compared with the predictions of the "time history modal superposition" analysis in Table IV. Specifically, it can be seen from this table that the highest percentage differences between the three "superposition of spectral responses" methods are 0% and +1.85% respectively for deformation in X and Y directions. Similarly, when one compares the mean values of the SRSS, CQC and ROSE methods with the predictions of the "time history based modal superposition" method, percentage differences are found as +9.37% and +4.5% for deformation in X and Y directions, respectively. The Finite element deformation maps for deformation in X and Y directions are presented in Figure 9.

*Table XII: MAXIMUM DEFORMATION STATE PREDICTIONS*

| Maximum Response | MAXIMUM DEFORMATION (mm) | | | | Highest % Difference of (A) wrt Mean of (A) | Highest % Difference of (B) wrt Mean of (A) |
|---|---|---|---|---|---|---|
| | Type (A) | | | Type (B) | | |
| | SRSS | CQC | ROSE | Transient | | |
| Deformation (x) | 0.29 | 0.29 | 0.29 | 0.32 | 0.00 | +9.37 |
| Deformation (y) | 0.036 | 0.035 | 0.035 | 0.037 | +1.85 | +4.50 |

The results obtained suggest that three approximate spectral response analysis techniques (SRSS, CQC and ROSE) show an upper bound variation of +1.82% for maximum stress/stress invariant and +1.85% for upper bound variation in the deformation state. When the mean maximum values obtained using the SRSS, CQC and ROSE methods are compared with the more rigorous time history based modal superposition approach, upper bound variations for stress/stress invariant are obtained as +7.26% while the upper bound variation for the deformation state are obtained as +9.37%. The results thus indicate that predictions of any one of the three approximate methods such as SRSS, CQC,& ROSE make predictions within a relative variance interval of less than about +2% for the stress & strain tensor, the stress invariants and the deformation vector.

However, when the results of the more accurate "time history based modal superposition" method are compared with the average predictions of the SRSS, CQC, & ROSE methods, it is found that the three approximate techniques underestimates the shear stress by as high as nearly 7.5% and overestimates the normal stress by nearly 5%. Similarly, the deformation response is underestimated by the approximate methods by as high as nearly 10%.

Thus it can be concluded that while either of the three approximate techniques of SRSS, CQC, & ROSE make mutually self consistent predictions for the stress & strain tensors and deformation vector, these techniques tend to significantly overestimate or underestimate these structural parameters with respect to the more accurate "time history based modal superposition" method. The results clearly show that any of the three approximate methods (SRSS, CQC and ROSE) can be used for quick seismic qualification of insulator bushings with a maximum loss of the accuracy of about ten percent.

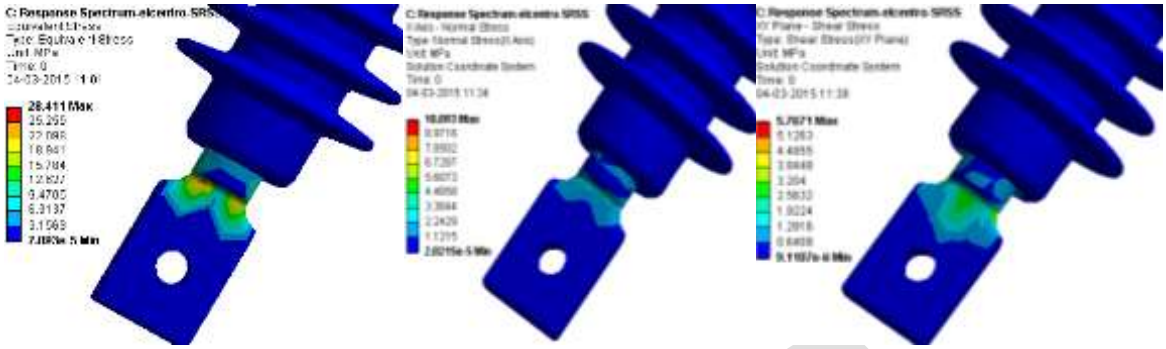

*Figure 6: Equivalent Stress, Normal Stress and Shear Stress using SRSS method*

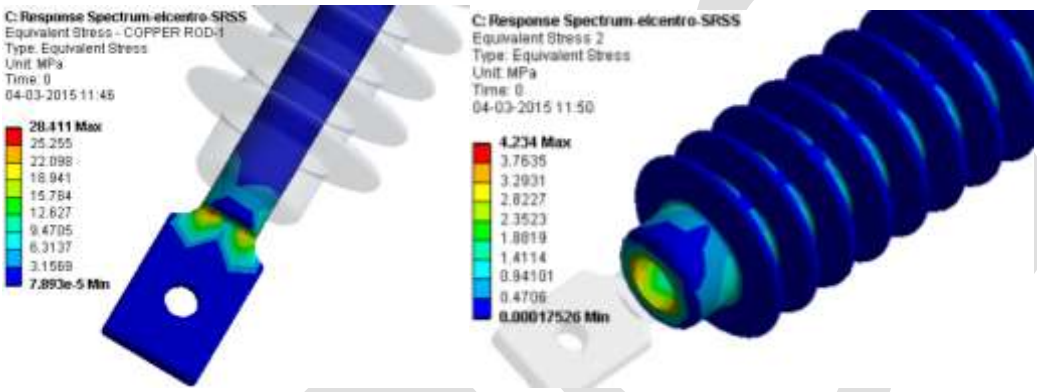


*Figure 7: Equivalent Stress Map in Copper conductor and ceramic bushing using SRSS method*

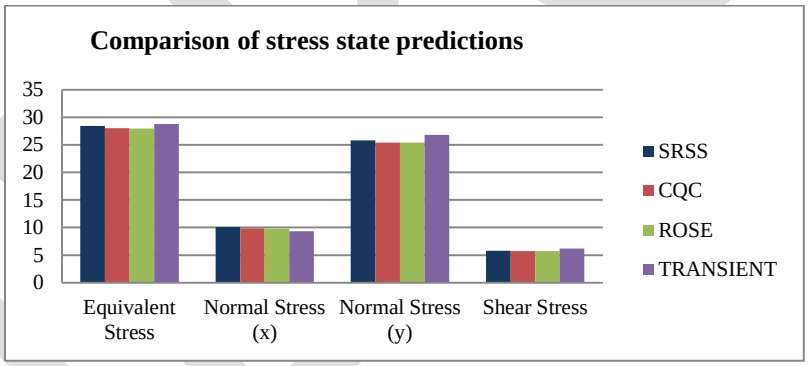


*Figure 8: Bar Graphs showing a comparison of stress state predictions*

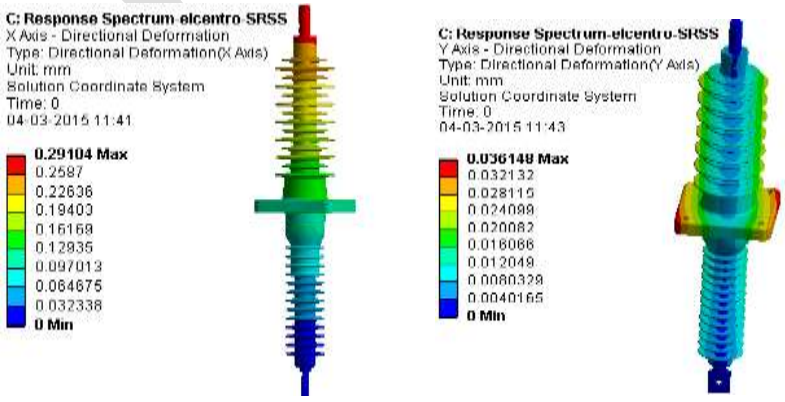


*Figure 9: Directional Deformation in X axes and Y axes obtained using SRSS method*

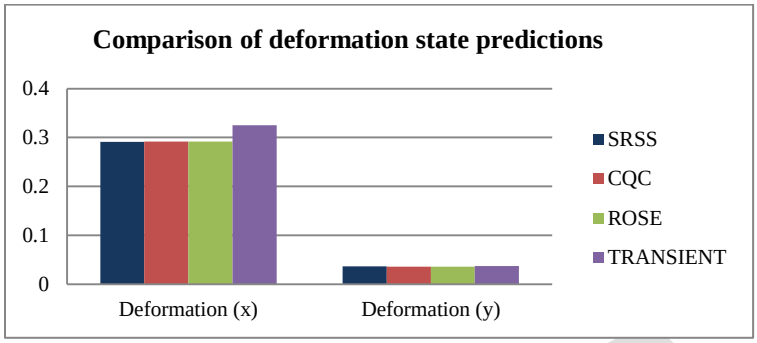


*Figure 10: Predictions of maximum deformation state for SRSS, CQC and ROSE as compared to the transient response method*

**ACKNOWLEDGMENT**

The authors would like to express their deepest gratitude to the Management of the Electrical Research and Development Association (ERDA) for providing technical and financial support for this study. Our sincere thanks also goes to the Department of Applied Mechanics, Faculty of Technology and Engineering (FTE), Maharaja Sayajirao University (MSU) of Baroda for supporting this study.

## CONCLUSION

Based on the results obtained, the following conclusions are derived:

1. The eigen-values of the insulator bushing are found to be uniformly distributed in the frequency space and do not show clustering, enabling the use of SRSS method of mode summation without loss of accuracy.
2. The response spectrum analysis was conducted using the acceleration spectra for the ELCENTRO (1940) earthquake using the SRSS, CQC and ROSE methods of mode summation. The Transient analysis was carried out using the actual ELCENTRO (1940) time history data.
3. The results obtained suggest that within themselves, the three approximate spectral response analysis techniques (SRSS, CQC and ROSE) show an upper bound variation of +1.82% for maximum stress/stress invariant and +1.85% for upper bound variation in the deformation state. Comparison of average predictions of SRSS, CQC and ROSE methods with the time history method indicate an upper bound variation of 7.26% for the maximum stress/stress invariant and an upper bound value of 9.37% for the maximum deformation.
4. Thus it can be concluded that while either of the three approximate techniques of SRSS, CQC, & ROSE make mutually self-consistent predictions for the stress & strain tensors and deformation vector, these techniques tend to significantly overestimate or underestimate these structural parameters with respect to the more accurate "time history based modal superposition" method.
5. The results suggest that any of the three approximate methods (SRSS, CQC and ROSE) can be used for quick seismic qualification of insulator bushings with a maximum loss of the accuracy of about ten percent.
6. The analysis indicates that the maximum stresses occur in the inner conductor of the insulator bushing, while the state of stressing in the brass bush and the porcelain casing are comparatively lower.

## REFERENCES:

[1] University of California, Electrical Grid Research, "Analysis of Seismic Performance of Transformer Bushings"
[2] Schiff A., "Guide to improved earthquake performance of electrical power systems", Rep. No. NIST GCR 98-757, National Institute of Standards and Testing, Washington, DC. 1998.
[3] Schiff. A. J, "Northridge Earthquake: Lifeline Performance And Post-Earthquake Response", Technical Council on Lifeline Earthquake Engineering; Monographs, ASCE, August 1995.
[4] Ibanez, P. Vasudevan, R. Vineberg, E. J., "A Comparison of Experimental Methods for Seismic Testing of Equipment", Nuclear Engineering and Design, 1973; 25:150-162.
[5] Ray W. Clough, Joseph Penzien (2003), "Dynamics of Structures", Third Edition, Computers & Structures, Inc.
[6] Bureau of Indian Standards, "Criteria for Earthquake Resistant Design of Structures, Part 4 Industrial Structures including Stack-like Structures", IS 1893(Part 4):2005.
[7] Rosenblueth E and Elorduy J., "Responses of Linear Systems to Certain Transient Disturbances," Proceedings of the Fourth World Conference on Earthquake Engineering, Santiago, Chile, 1969.
[8] Der Kiureghian A, "A Response Spectrum Method for Random Vibrations," University of California, Berkeley, June 1980.
[9] Anil K Chopra (2007), "Dynamics of Structures, Theory and Application to Earthquake Engineering", Third Edition, Pearson.
[10] ANSYS, ANSYS 14.5, Analysis Guide